Journal of Low Temperature Physics, Vol. 109, Nos. 1/2, 1997

Magnetic Correlations in $Ce_{0.925}La_{0.075}Ru_2Si_2$

S. Raymond,[1,*] L. P. Regnault,[1] S. Kambe,[1] J. M. Mignot,[2] P. Lejay,[3] and J. Flouquet[1]

[1]*CEA—Département de Recherche Fondamentale sur la Matière Condensée, SPSMS/MDN 38 054 Grenoble Cedex 9, France*
[2]*Laboratoire Léon Brillouin, CEA-CNRS, Centre d'Etudes de Saclay, 91 191 Gif sur Yvette Cedex, France*
[3]*Centre de Recherche sur les Très Basses Températures, CNRS, BP 166, 39 042 Grenoble Cedex 9, France*

(Received February 17, 1997; revised May 7, 1997)

Inelastic neutron scattering experiments were performed to study the spin dynamics of the heavy fermion compound $Ce_{0.925}La_{0.075}Ru_2Si_2$. This composition corresponds to the borderline of the magnetic-non magnetic transition in the family of alloys $Ce_{1-x}La_xRu_2Si_2$. Short range magnetic correlations of an inelastic nature characterize this system in addition to a small ordered moment of the order of $0.02\mu_B$ which appears below 2 K. Comparison with the magnetic excitation spectrum of the Pauli paramagnet $CeRu_2Si_2$ is given from the viewpoint of recent work on phase transitions near the magnetic instability point.

1. INTRODUCTION

Heavy fermion systems are rare earth or actinide intermetallic compounds near a magnetic instability and driven by the competition between the Kondo effect and the RKKY interactions. These compounds take their name from the observation, at low temperature, of a Fermi Liquid (FL) ground state with large effective masses. Among these compounds the family $Ce_{1-x}La_xRu_2Si_2$, allows the opportunity of crossing the Magnetic-Non Magnetic (M-NM), transition.[1,2] The ground state is driven by the concentration x ranging from a Pauli Paramagnet for $x < 0.08$ to an antiferromagnet for $x > 0.08$. Recently interest in this topic has been revived, with the experimental emphasis on Non Fermi Liquid behaviour (NFL) of a certain class of compounds (e.g. $CeCu_{6-x}Au_x$[3] and $U_xY_{1-x}Pd_3$[4]), for critical concentration x_c corresponding to the M-NM

*Temporary address: Brookhaven National Laboratory, Bldg 510B, Upton, New York 11973, USA.

0022-2291/97/1000-0205$12.50/0

transition. A recent theoretical review[5] summarizes the phase diagram around the $T=0$ K phase transition using the Renormalisation Group (RG) approach. The main idea is that when driving the transition temperature to zero, dynamic and static correlations are mixed due to quantum effects leading to a specific critical behaviour. Another method, based on the Self Consistent Renormalized (SCR) Spin Fluctuation (SF) theory,[6] describes the properties of these systems starting from the spin dynamics and taking into account the evolution of the characteristic energy width and correlation length across the M-NM transition line. The physical properties of the compound $Ce_{1-x}La_xRu_2Si_2$ for $x=0$, 0.05 and 0.075 were interpreted in this framework[7] and Inelastic Neutron Scattering (INS) results, which probe the spin dynamics, were used in order to support this interpretation.

In this paper we give the details of the INS experiments carried out for $x=0.075$. Previous INS studies were mainly carried out on the pure paramagnetic compound $CeRu_2Si_2$.[8] Here, the magnetic excitation spectrum shows the existence of antiferromagnetic correlations peaked at the wave vectors $\mathbf{k}_1=(0.31, 0, 0)$ and $\mathbf{k}_2=(0.31, 0.31, 0)$. These excitations are inelastic in nature with a characteristic energy $\omega_0=0.5$ meV for $\mathbf{k}_1$ and $\omega_0=1.2$ meV for $\mathbf{k}_2$. The damping of these modes has a magnitude of $\Gamma_{IS}=0.75$ meV. The intensity associated with these excitations collapse at the metamagnetic field $H=8$ T[9,10] while a second local contribution persists at high magnetic field. This latter **Q** independent contribution is associated with local single site magnetic fluctuations and is quasielastic in nature with an energy width $\Gamma_{SS}=2$ meV. The wavevector $\mathbf{k}_1$ becomes the propagation vector of an ordered magnetic structure for the compounds with x larger than the critical value $x_c=0.08$.[11]

2. EXPERIMENTAL DETAILS

$CeRu_2Si_2$ crystallizes in the body centred tetragonal I4/mmm space group with the lattice parameters $a=b=4.197$ Å and $c=9.797$ Å. The evolution of these parameters with the La concentration is roughly linear and on the order of 5.10^{-4} Å/at.% La.[12] The crystal studied with $x=0.075$, grown by the Czochralsky method,[13] has a typical volume of 250mm^3. The concentration precision is of the order of 0.0125% which is established by the variation of the physical properties of several crystals grown by varying the starting compositions in incremental steps. Experiments were carried out on several Three Axis Spectrometers (TAS). Preliminary experiments were performed on the thermal TAS DN1 installed at CEN-Grenoble for each direction *a*, *b* and *c*. Qualititavely, these measurements showed that the physics of this compound follow the behaviour expected for the entire

family. However, it appeared obvious that measurements with an improved energy resolution were necessary due to the energy narrowing of the spin dynamics for $x = 0.075$. The main experiments were performed on the cold TAS IN12 at the ILL-Grenoble and the cold TAS 4F2 at LLB-Saclay. In all cases we worked in the constant final momentum energy mode using $k_F = 1.55$ Å^{-1}. Pyrolityc graphite monochromators and analysers were used in both experiments. No filter was used neither on IN12 nor on 4F2 because we mainly worked at the incommensurate position where the effects of higher order contamination are minimized. Moreover on IN12, the contamination is reduced by the guide curvature. On this spectrometer, the neutron beam was collimated with 40′-sample-60′-60′ yielding a typical Full Width at Half Maximum (FWHM) of the incoherent signal of 0.15 meV. For the 4F2 spectrometer, we used a horizontally focusing analyser and no collimation which leads to a slightly larger FWHM of the incoherent signal of 0.2 meV. We verified that the degradation of the resolution in **Q** due to the horizontal focalization is not a problem. This is because the **Q** extend of the spectrum of this compound is large compared to the resolution. The easy c-axis was vertical and the scattering plane was the (a, b) plane. Two kind of low temperature devices were used: a standard ^{4}He flow cryostat reaching 1.5 K was used on both spectrometers and additional measurements at very low temperatures were done on IN12 using a dilution refrigerator. The sample was mounted in an aluminium can filled with helium. The minimum temperature reached on the mixing chamber was 50 mK. However the loss of signal and the strong contamination due to roton excitations in liquid helium-4 seriously limited our studies.

3. ELASTIC SCATTERING

Elastic scattering performed on a TAS is a powerful method to determine small magnetic moments because Bragg scattering can be discriminated from low energy excitations by setting the analyser to zero energy transfer. **Q** scans performed at zero energy transfer around the wavevectors $\mathbf{k}_1$ and $\mathbf{k}_2$ reveal the existence of magnetic elastic scattering for the wavevector $\mathbf{k}_1$ which is surprising for this composition since no magnetic ordering is expected for $x = 0.075 < x_c = 0.08$. A typical **Q** scan is shown in Fig. 1a at 50 mK. At the lowest temperature, the lineshape is slightly broader than the instrumental resolution. As a consequence the spectrum looks like gaussian but it is much better accounted by a Lorentzian lineshape convoluted with the Gaussian resolution in the scan direction. As the temperature is increased the spectrum broadens slightly in the range 50 mK–1.5 K and broadens considerably above 1.5 K as shown comparatively in Fig. 1b for **Q** scans performed 1.5 and 2.5 K. The Lorentzian

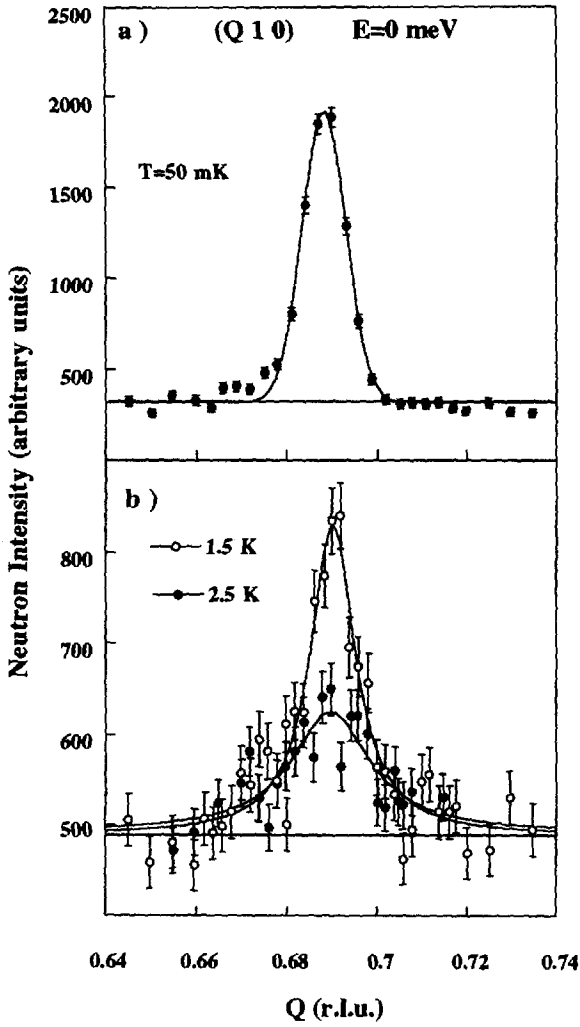

Fig. 1. (a) Constant energy scan performed at $E=0$ meV at 50 mK on IN12 at $k_F=1.55$ Å^{-1}. The line is a fit with a gaussian lineshape slightly larger than the resolution. (b) Constant energy scan performed at $E=0$ meV at 1.5 and 2.5 K. The line is a fit with a Lorentzian lineshape.

lineshape used in the whole temperature range indicates the occurrence of some disorder. These data are consistent with the existence of a transition toward a phase which exhibits long range magnetic ordering associated with a tiny moment. The maximum intensity of the magnetic Bragg peak versus temperature is shown in Fig. 2 after subtraction of the background.

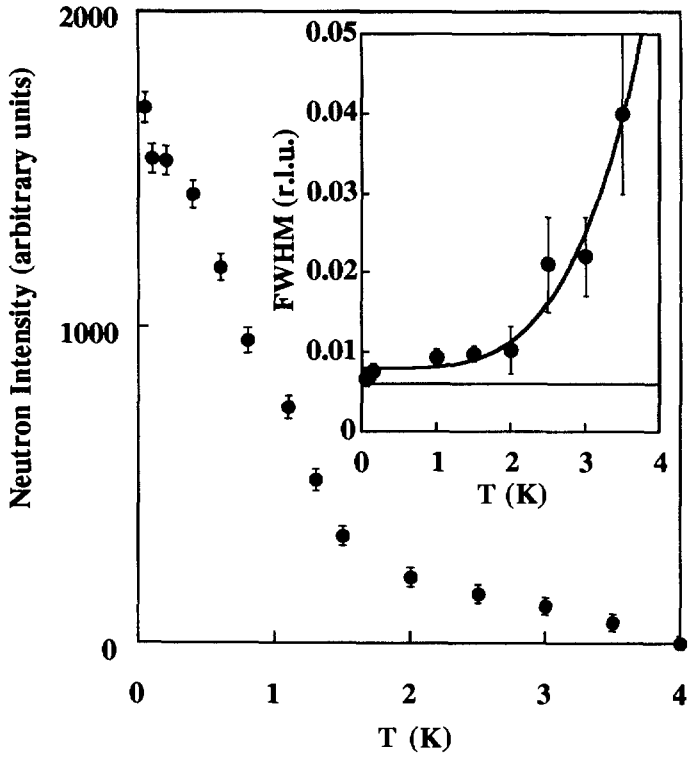

Fig. 2. Temperature dependence of the maximum elastic intensity at $\mathbf{Q} = (0.69\ 1\ 0)$ (The incoherent background is substracted). The inset shows the FWHM of the peak versus temperature. The line is a guide to the eyes. The horizontal line indicates the resolution. Measurements were done on IN12 at $k_F = 1.55$ Å^{-1}.

This curve is composed of two linear parts. The first one is associated with the Bragg component of the signal from 50 mK to 1.5 K whereas the second one is associated with some kind of diffuse scattering in the range 2–3 K. The intersection of these two parts gives a Néel temperature of $T_N = 1.8$ K which is correlated with the saturation of the FWHM of the magnetic Bragg peak shown in the inset of Fig. 2. At the lowest temperature the correlation length, defined as the inverse of the Lorentzian FWHM, reaches 200 Å. The intensity is not saturated at $T = 50$ mK and corresponds to an ordered magnetic moment of about $0.02\mu_B$ determined by comparison with the weak nuclear Bragg peak (1 1 0). The quantities $m = 0.02\mu_B$ and $T_N = 1.8$ K are not consistent with the reported phase diagram for $x > 0.08$ of $Ce_{1-x}La_xRu_2Si_2$[11] and shown in Fig. 3. For example

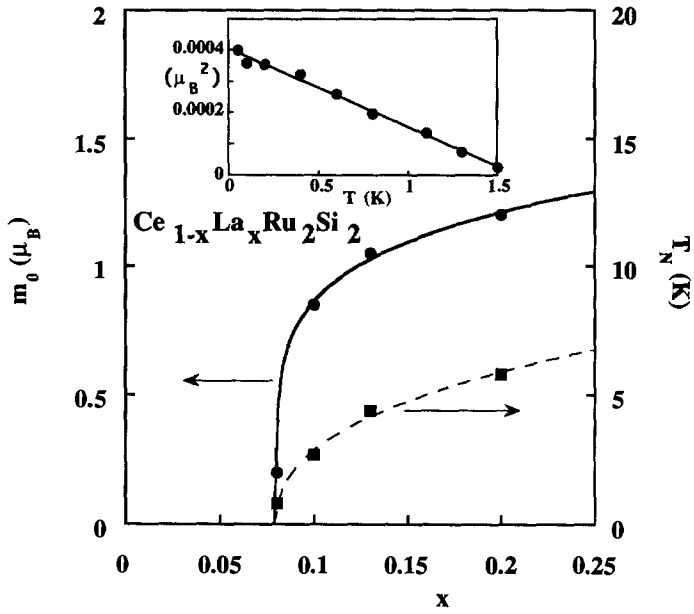

Fig. 3. Néel temperature and saturated momentum versus the lanthanum concentration x. The inset shows the best fit of $I(T)$ for $x = 0.075$ with the model described in the text.

at $x = 0.08$ the values determined by neutron scattering are $T_N = 0.8$ K and $m = 0.2\mu_B$. This discrepancy (the ordered moment is too small for such a Néel temperature) as well as the observation of a magnetic moment for a concentration where the system was believed to be paramagnetic lead us to make at least two hypotheses. The first one, based on the observation of a tiny ordered moments phase in UPt_3 ($m = 0.02\mu_B$, $T_N = 5$ K)[14] and URu_2Si_2 ($m = 0.04\mu_B$, $T_N = 17.5$ K),[15] is to consider the behaviour reported here as intrinsic to the existence of a tiny ordered moment phase in $Ce_{1-x}La_xRu_2Si_2$ for $x < 0.08$. This may be linked with the observation of a static moment of $10^{-3}\mu_B$ in the pure compound $CeRu_2Si_2$ by μSR experiments[16] below $T = 2$ K. The evolution from a small moment phase to a phase displaying conventional magnetic order also occurs for the family $U(Ru_{1-x}Rh_x)_2Si_2$.[17] In this family conventional long range order appears for $x > 0.4$ with a moment of the order of $2\mu_B$ and a Néel temperature of about 150 K whereas for $x < 0.06$ the moment is $0.04\mu_B$ and T_N of about 20 K. The same scenario applies for $U(Pt_{1-x}Pd_x)_3$ where the concentration $x = 0.01$ seems to indicate a crossover behaviour from small moment ($x \to 0$) to large moment antiferromagnetic order.[18] A second hypothesis is

to consider this behaviour as a consequence of disorder induced by doping. If there is a distribution of concentration in the sample (e.g. clusters with $x > 0.08$), it is possible to have such a behaviour. We take the data for $x = 0.08$, 0.1, 0.13 and 0.2[11] and fit the moment and the Neél temperature versus x with power laws often used to describe critical behaviour but we use these expressions over a large range of concentration. The moment is fit by:

$$m_0 = A\left(\frac{x}{x_c} - 1\right)^{\alpha_m} \tag{1}$$

with $A = 1.1\mu_B$, $x_c = 0.08$ and $\alpha_m = 0.2$. The Néel temperature versus x was fit by

$$T_N = B\left(\frac{x}{x_c} - 1\right)^{\alpha_T} \tag{2}$$

with $B = 5$ K, $x_c = 0.08$ and $\alpha_T = 0.4$. These fits are shown in Fig. 3. Then the magnetic moment is written as:

$$m(T) = \int_0^{x_M} m_0(x)\left(1 - \frac{T}{T_N(x)}\right)^{\beta(x)} g(x - x_c)\, dx \tag{3}$$

where x_M is the integration limit ($x_M = 0.25$) and g is a distribution function peaked at the nominal La content of our sample $x_c = 0.075$ and assumed to be Gaussian:

$$g(x) = \frac{1}{\sigma\sqrt{2\pi}} e^{-x^2/2\sigma^2} \tag{4}$$

β is taken independent of x and equal 0.5 because the compound is located in the vicinity of a $T = 0$ K phase transition where the mean field exponents are expected to describe the system.[5] The integration is performed over the range $0 < x < 0.25$ because g is considered to be zero outside of this interval. The result of the fit using expression (3) is shown in the inset of Fig. 3. σ is the only fitted parameter; we find $\sigma = 0.0025$ a value which quantitatively confirms the good quality of our sample. In this picture only the points obtained below 1.5 K when the correlation length diverge are considered. A mean concentration $x = 0.075 \pm 0.0025$ accounts well for the behaviour observed. We note that this good agreement is stable against small changes in the chosen parameters in Eqs. (1)–(3). Such a distribution of concentration can have a chemical origin, e.g. during the crystal growth.

Another possibility is to consider the formation of clusters driven by electronic phenomena. This picture is extensively studied for the high T_c superconductors, which exhibit a transition from an antiferromagnetic to a superconducting state with increasing oxygen content. Such a phase separation is theoretically expected for the $t-J$ model as well as for the Kondo lattice model also used for heavy fermion systems.[19] The main physical idea is that it is favourable to create magnetic clusters in a non magnetic host in order to maximize the gain in exchange energy. More experiments are needed to give a definitive conclusion on intrinsic or disorder nature of the weak ordered moment. The magnetic ordering reported is not observed in resistivity nor in specific heat measurements.[7]

4. INELASTIC NEUTRON SCATTERING

4.1. Inelastic Neutron Scattering at 1.5 K

The spin dynamics was studied at 1.5 K around the wave vectors $\mathbf{k}_1$ and $\mathbf{k}_2$ where the magnetic correlations peak. Typical $\mathbf{Q}$ scans performed at 0.25 meV at 1.5 K are shown in the inset of Fig. 4. These data exhibit a typical lineshape characteristic of short range correlations. The background of the spectrometer determined at negative energy transfer does not correspond to the background of the $\mathbf{Q}$ scans which is defined by the flat part of the lineshape. This is the signature of a single site (or $\mathbf{Q}$ independent) contribution to the magnetic cross section[9, 10] in addition to the correlated part. Energy scans performed at $\mathbf{Q}=\mathbf{k}_1$ and $\mathbf{Q}=\mathbf{k}_2$ at 1.5 K are shown in Fig. 4. The lineshape is characteristic of a damped response. In principle, $\mathbf{k}_1$ is the relevant vector to study the critical behaviour of the compound since it is the ordering vector. But, as shown in Fig. 4, the spectra are almost identical and both wave vectors are suitable to study the characteristic dynamics of the compound. Since the studies on $\mathbf{k}_2$ are easier to perform because the peaks in $\mathbf{Q}$ space are more widely spaced, we studied principally this vector.

For a quantitative analysis of the data, we used a cross section which describes the entire magnetic excitation spectrum.[9, 10, 20] The intensity is written $I(\mathbf{Q}, \omega) = I_{BG} + (1 + n(\omega))(\chi''_{SS}(\omega) + \chi''_{IS}(\mathbf{Q}, \omega))$ where I_{BG} is the background neutron intensity, $n(\omega)$ is the bose factor and χ''_{SS} and χ''_{IS} are respectively the imaginary part of the single site and intersite magnetic dynamical susceptibility. The $\mathbf{Q}$ independent part is assumed to be Lorentzian reflecting local $4f$ spin relaxation. We used the form:

$$\chi''_{SS}(\omega) = \chi_{SS} \frac{\omega \Gamma_{SS}}{\omega^2 + \Gamma_{SS}^2} \tag{5}$$

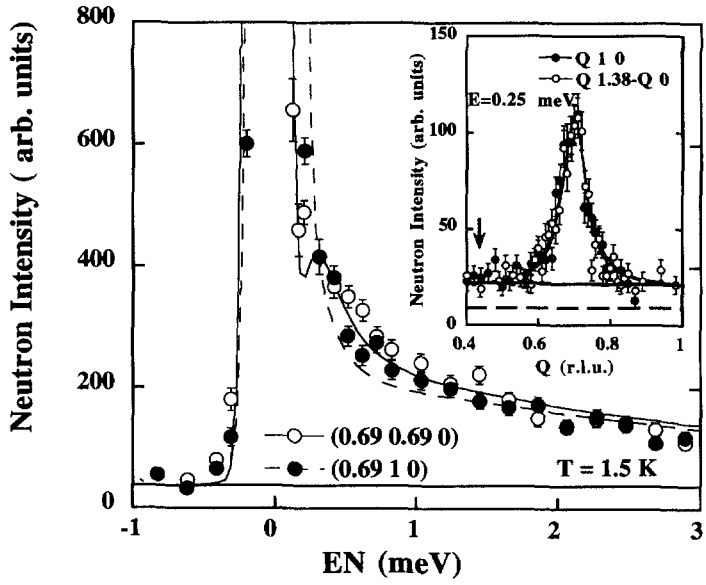

Fig. 4. Energy scan performed at $\mathbf{Q}=(0.69\ 0.69\ 0)$ and $\mathbf{Q}=(0.69\ 1\ 0)$ at 1.5 K. Measurements were done on 4F2 at $k_F=1.55$ Å^{-1}. The dotted and respectively the solid lines are the best fit including the incoherent signal, the single site and the intersite contributions for respectively $\mathbf{k}_1$ and $\mathbf{k}_2$. The inset shows a $\mathbf{Q}$ scan performed at $E=0.25$ meV at 1.5 K around $\mathbf{k}_1$ and $\mathbf{k}_2$ on IN12. Two background levels are indicated: The full line corresponds to the local contribution, the dotted line is the background determined at negative energy transfer. The arrow indicates the wavevector where the single site contribution is studied.

For the correlated signal, we used the following formula where $\mathbf{q}$ is the wave vector of the excitation $\mathbf{q}=\mathbf{Q}-\mathbf{k}_1$ and $\mathbf{q}=\mathbf{Q}-\mathbf{k}_2$ and making the isotropic approximation, we write:

$$\chi''_{IS}(q,\omega)=\chi_{IS}(q)\,\omega\,\frac{1}{2}\left[\frac{\Gamma_{IS}(q)}{\Gamma_{IS}(q)^2+(\omega-\omega_0(q))^2}+\frac{\Gamma_{IS}(q)}{\Gamma_{IS}(q)^2+(\omega+\omega_0(q))^2}\right] \tag{6}$$

The simplest approximation, compatible with antiferromagnetic like correlations for $\chi_{IS}(q)$ and $\Gamma_{IS}(q)$ are:

$$\chi_{IS}(q)=\frac{\chi_{IS}(0)}{1+(q/\kappa)^2} \tag{7}$$

$$\Gamma_{IS}(q)=\Gamma_{IS}(0)(1+(q/\tau)^2) \tag{8}$$

The static susceptibility is linked to the dynamical one through the Kramers Kronig relation:

$$\chi'_{IS}(q) = \int \frac{\chi''_{IS}(q, \omega)\, d\omega}{\omega} \tag{9}$$

In relation (7) and (8), κ is the inverse correlation length and τ is characteristic of the q dependence of the energy width. Equation (6), which is often used in the analysis of INS data, has no physical basis and is purely phenomenological. We use it rather than the harmonic oscillator in order to compare our results with previous work[8–10, 20] Generally, the double Lorentzian lineshape is usually used to describe critical scattering data whereas the harmonic oscillator is used to describe dynamical modes in a continuous broken symmetry phase.[21]

The **Q** independent part is determined at the scattering vector $\mathbf{Q} = (0.44\ 1\ 0)$ where the spin correlations vanish as shown by the arrow in the inset of Fig. 4. The local fluctuations give rise to a quasielastic lineshape with a characteristic width $\Gamma_{SS} = 1.4$ meV. This energy scale is commonly associated with the Kondo temperature since the Kondo effect is the single site process which gives rise to the $4f$ moment relaxation. Concerning the correlated part, a different behaviour occurs for $\mathbf{k}_1$ and $\mathbf{k}_2$. The analysis of the data using formula (6) shows that, for the first wave vector, the fluctuations are quasielastic ($\omega_0 = 0$ meV), which is consistent with the fact that this wave vector is the propagation vector of the ordered structure; the value of the width is $\Gamma_{IS} \approx 0.2$ meV. For the second wavevector, there is a characteristic energy $\omega_0 \approx 0.2$ meV with a damping $\Gamma_{IS} \approx 0.2$ meV. In the analysis of the data the **Q** independent contribution was fixed and only the correlated part of the signal has been fitted. For the first wavector an additional contribution corresponding to the Bragg peak has also been taken into account; that is why the energy width around zero energy transfer is larger for $\mathbf{k}_1$. The characteristic energies determined are shown comparatively for $x = 0$ and $x = 0.075$ in Table I. The main result, emphasizes in Table I, is the strong decrease of the intersite energies Γ_{IS} by a factor 4 and ω_0 by a factor 6 for $x = 0.075$ compared with $x = 0$.

TABLE I

Characteristic Parameters of the Spin Dynamics for $\mathbf{k}_2$ at 1.5 K

	Γ_{SS} (meV)	Γ_{IS} (meV)	ω_0 (meV)
$x = 0$	2.0 (1)	0.75 (5)	1.2 (1)
$x = 0.075$	1.4 (1)	0.20 (5)	0.2 (1)

In order to study the q dependence of the magnetic excitation spectrum around $\mathbf{k}_2$, we performed energy scans at the wave vectors $\mathbf{Q} = (0.69 - q, 0.69 + q, 0)$ with $q = 0.03$, 0.05, 0.08 at 1.5 K. Some of these spectra are shown in Fig. 5. The main feature is the broadening of the energy width with q. The single site signal determined at $\mathbf{Q} = (0.44\ 1\ 0)$ is also shown. For the analysis of the data this contribution and the incoherent signal are kept fixed. Two analysis can be performed. The first one which gives the best fit is obtained if ω_0 is q dependent (varying between 0.2 and 0.4 meV in the q range studied); in this case $\chi_{IS}(q)\,\Gamma_{IS}(q)$ decreases slightly when q increases. The second fit involves fixing the value of ω_0 equal to 0.2 meV. In this case, we find that $\chi_{IS}(q)\,\Gamma_{IS}(q)$ is constant (this is often assumed in theoretical works[22]). The parameters extracted from the two analysis are given respectively in Table II.1 and II.2. As it is difficult to determine precisely ω_0, because it is of the order of the damping Γ_{IS}, and without any model so far, we use the second analysis which is simpler for the discussion. Therefore, when using formulas (7) and (8) $\kappa = \tau$. The correlation length is derived from the amplitude $\chi_{IS}(q)$ of the

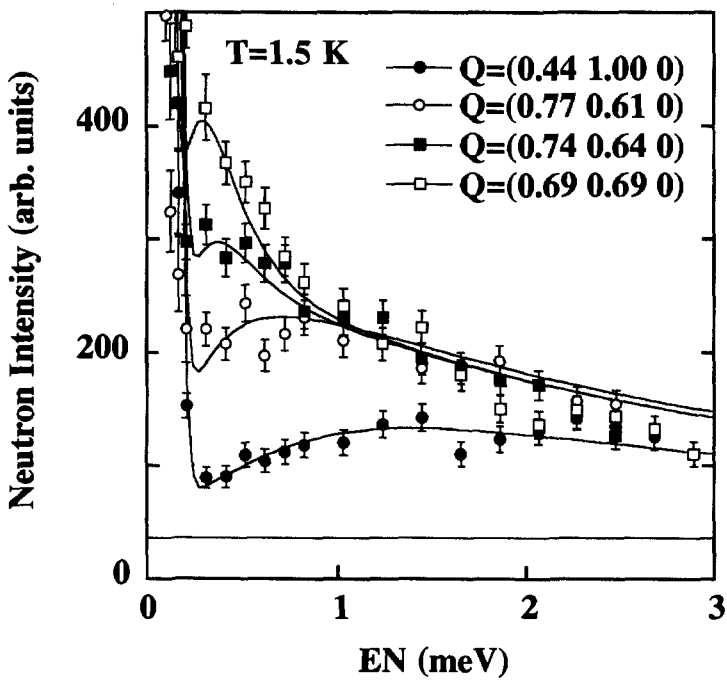

Fig. 5. Energy scans performed at $\mathbf{Q} = (0.69 + q\ \ 0.69 - q\ \ 0)$ and $\mathbf{Q} = (0.44\ 1\ 0)$ at 1.5 K on 4F2. The full line corresponds to the fit indicated in the text.

TABLE II.1

Parameters Deduced from (6) Without Any Assumption

	$q=0$	$q=0.03$	$q=0.05$	$q=0.08$
$\chi_{IS}(q)$ (a.u)	740 (40)	542 (40)	404 (40)	240 (40)
$\Gamma_{IS}(q)$ (meV)	0.17 (5)	0.22 (5)	0.25 (5)	0.36 (5)
$\chi_{IS}(q)\,\Gamma_{IS}(q)$	1.1 (2)	0.9 (2)	0.8 (2)	0.7 (2)
$\omega_0(q)$ (meV)	0.2 (1)	0.3 (1)	0.3 (1)	0.4 (1)

energy scans performed at $\mathbf{Q}=(0.69-q, 0.69+q, 0)$. It is defined as $\xi=a/(2\pi\kappa)$ and is found to be of the order of 11.5 Å which corresponds to 2.7 lattice parameters. This is of the order of 1.5 times higher than in the pure compound. This analysis based upon the Lorentzian assumption (5)–(8) is also supported by **Q** scans performed at constant energy transfer $E=0.25$, 0.41, 0.7 meV which can be described without additional parameters.

4.2. Temperature Dependence of the Magnetic Excitations

In this part we describe the effect of the temperature on the parameters and compare these results with those previously obtained on the pure compound. Concerning scans performed at constant energy transfer, from which we want to extract a correlation length, we proceed in two ways (we exclude in this analysis the contribution from the magnetic elastic Bragg peak). The first analysis considers a characteristic length ξ' which is obtained by performing a scan around $\mathbf{k}_2$ at a constant energy transfer equal to ω_0. Such scans are shown in Fig. 6. The main feature is the broadening of the peak with the temperature. The background, which is linked to the single site contribution, increases with the temperature in agreement with the energy scans performed at $\mathbf{Q}=(0.44\ 1\ 0)$ at various temperatures. The analysis of the lineshape with the formula (7), used as a

TABLE II.2

Parameters Deduced from (6) with the Assumption $\omega_0=$const.

	$q=0$	$q=0.03$	$q=0.05$	$q=0.08$
$\chi_{IS}(q)$ (a.u)	740 (40)	542 (40)	444 (40)	270 (40)
$\Gamma_{IS}(q)$ (meV)	0.20 (5)	0.22 (5)	0.32 (5)	0.50 (5)
$\chi_{IS}(q)\,\Gamma_{IS}(q)$	1.0 (2)	0.9 (2)	1.1 (2)	1.1 (2)
$\omega_0(q)$ (meV)	0.2	0.2	0.2	0.2

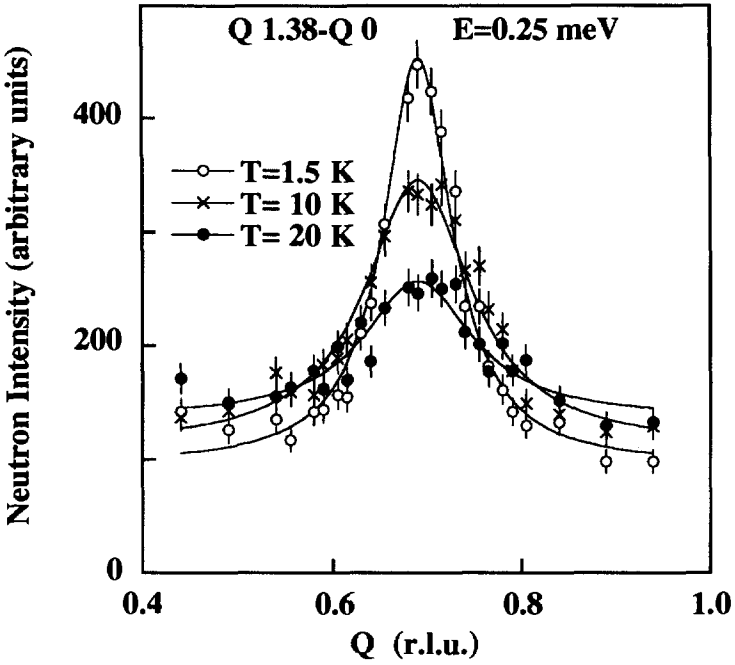

Fig. 6. Constant energy scans performed at $E = 0.25$ meV at 1.5, 10 and 20 K on 4F2. The full line is a fit to a Lorentzian profile.

fit function to describe $\chi''(q, \omega_0)$, defines the quantity ξ'. This characteristic length reflects the correlation length ξ and is nearly equal to ξ when the spectrum is broad. This quantity ξ' is directly comparable with previous measurements performed on the pure compound $CeRu_2Si_2$ at $\omega_0 = 1.6$ meV. In the case of the Lorentzian approximation with $\chi_{IS}(q)\,\Gamma_{IS}(q) = \text{constant}$, which seems to be verified in our compound, the correlation length is defined in formula (7) and equals $\xi = a/(2\pi\kappa)$. Performing this analysis, we found approximately $\xi' = 1.5\xi$. It is obvious that the error bars, due to the weak statistics of the data, exclude in fact a fine treatment so that each quantity ξ or ξ' is pertinent in order to describe the spin dynamics in this compound. (We recall that the real correlation length is obtained by integrating in energy the scattering function $S(\mathbf{Q}, \omega)$ instead of the susceptibility. This gives an instantaneous scattering function $S(\mathbf{Q})$. The q width around $\mathbf{Q} = \mathbf{k} + \mathbf{q}$ gives the correlation length.We must notice that the correlation length determined either by the instantaneous scattering function or the susceptibility are different because of the bose factor). As shown in Fig. 7, for $x = 0.075$, the length ξ' increases when the temperature

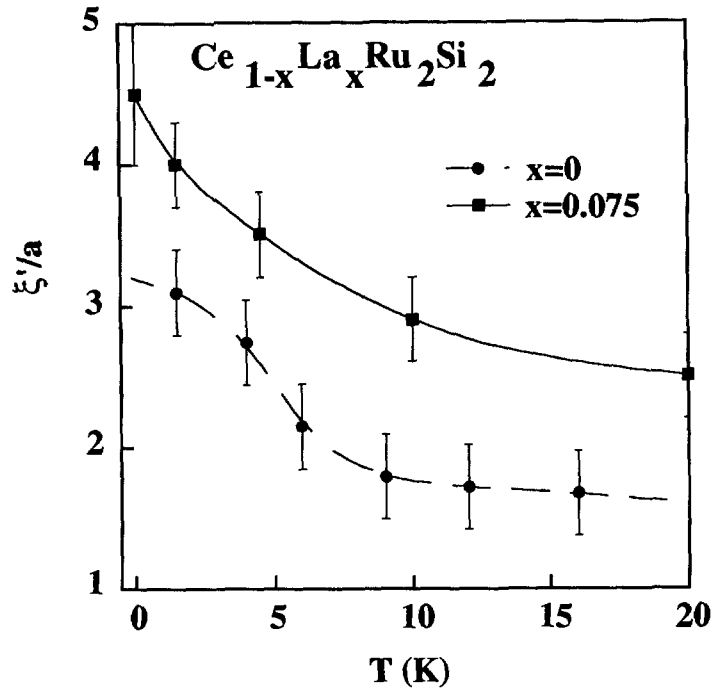

Fig. 7. Temperature dependence of the magnetic correlation length for $x=0$ (circles) and $x=0.075$ (squares). Lines are guide to the eyes.

decreases and its saturation is not well established. Nevertheless this increase attenuates itself and an inflexion point may occur below 1 K. On the contrary, for the pure compound, the correlation length seems to saturate below 2 K. This behaviour will be discussed in the next section in connection with the location of each compound in the magnetic phase diagram of $Ce_{1-x}La_xRu_2Si_2$.

The temperature dependence of the different energy widths was also studied. We performed energy scans at $\mathbf{Q}=(0.44, 1, 0)$ and $\mathbf{Q}=\mathbf{k}_1$ at 1.5, 4.5, 10 and 20 K. The quantities Γ_{IS}, Γ_{SS} are given in Fig. 8. The quantity Γ_{IS}, obtained for $x=0$, is plotted for comparison. Concerning the intersite width Γ_{IS}, the striking point is the decrease of the energy scale for $x=0.075$, while the T dependence is similar and approximately linear for both compositions. The temperature dependence of the local energy width Γ_{SS} is compatible with the typical $\sqrt{T}$ behaviour which is observed in other heavy fermion or intermediate valence compounds.[23] On another hand in the pure compound this energy width Γ_{SS} (not shown in Fig. 8) is

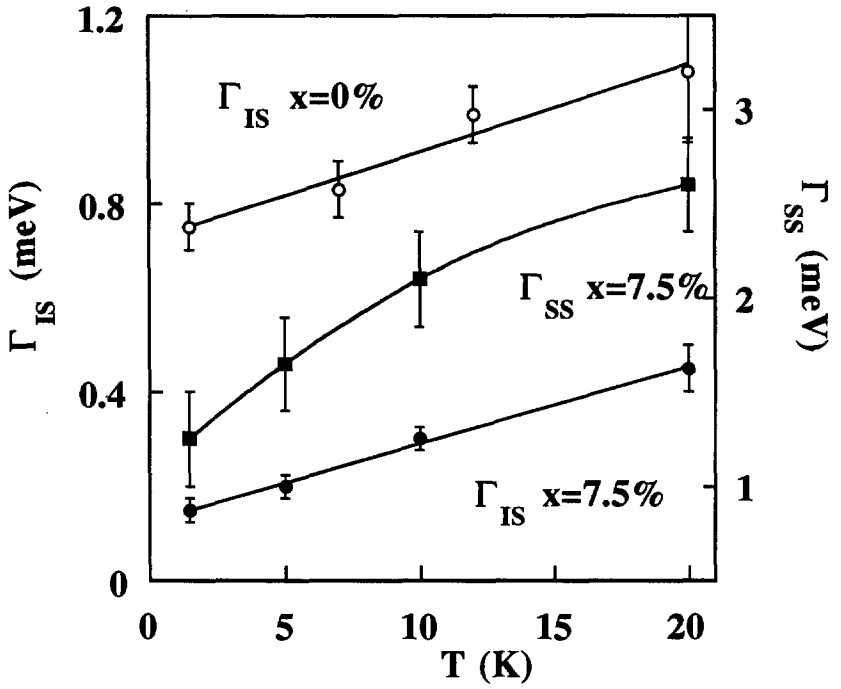

Fig. 8. Temperature dependence of the single site and intersite energy width for $x = 0.075$ (full symbols). The intersite width of the pure compound is represented for comparison (empty circles). Lines are guides to the eyes.

almost constant in this range of temperature and equals 2 meV; it is only at 40 K that this quantity becomes temperature dependent. The difference between the temperature dependence of Γ_{SS} in the two compounds is understood from a scaling between Γ_{SS} and the temperature at which this quantity is temperature dependent. The behaviour of the two compounds with $x = 0$ and $x = 0.075$ is discussed in the next part in the framework of the SCR theory.

4.3. Discussion

1. Data Analysis: Single Site and Intersite Contributions

As discussed above, the susceptibility is described by the sum of a **Q** independent contribution and a correlated part. The advantage of this approach is to describe the magnetic excitation spectrum over the entire Brillouin zone using simple analytic lineshapes. In the first works on

$CeRu_2Si_2$,[8] the single site contribution was not taken into account since only high magnetic field studies unambiguously underline the existence of this contribution.[9,10] By applying a magnetic field, the correlated part of the dynamical susceptibility vanishes due to the collapse of the RKKY interactions and only the single site contribution persists. That is why we rule out, in this paper, the possibility that what we call the single site signal is only extra intensity coming from an overlap of the peaks located at $\mathbf{k}_1$ and $\mathbf{k}_2$. Moreover in the compound studied here, the peaks are sharper, this overlap is smaller and less likely to lead to a misinterpretation of the data. On another hand this phenomenological separation in two parts of the signal, used without any theoretical model so far, has a drawback. The characteristic length and energy extracted from formula (6)–(8) are different from the one used in theoretical approaches. In theoretical studies,[6,22] the dynamic susceptibility is computed in the Random Phase Approximation (RPA) and is written in the form:

$$\chi(\mathbf{Q}, \omega) = \frac{\chi_{SS}(\omega)}{1 - J(\mathbf{Q})\,\chi_{SS}(\omega)} \tag{10}$$

The interest of this expression is to clearly show that the single site response is enhanced by the magnetic interactions giving a physical interpretation of the spectrum without arbitrarily separating the single site and intersite responses. The drawback of (10) is that the expression of $J(\mathbf{Q})$ is not obvious. Without a model, we can separate the Brillouin zone in two areas. In the first one close to $\mathbf{k}_1$ and $\mathbf{k}_2$, $J(\mathbf{Q})$ is expended as $J(\mathbf{Q}) = J(\mathbf{k}) + A\mathbf{q}^2$; this part describes the correlated signal. In the second area, sufficiently far from $\mathbf{k}_1$ and $\mathbf{k}_2$, $J(\mathbf{Q}) = 0$ which describes the single site signal. Unfortunately, the analysis of the data with formula (6)–(8) or with formula (10) does not give the same physical parameters (correlation length and energy width). This is clear when rewriting (10) as the sum of a single site and an intersite signal:

$$\chi(\mathbf{Q}, \omega) = \chi_{SS}(\omega) + \frac{\chi_{SS}^2(\omega)\,J(\mathbf{Q})}{1 - J(\mathbf{Q})\,\chi_{SS}(\omega)} \tag{11}$$

If we expand the second term of (11) in order to compare it with $\chi''_{IS}(\omega)$ given in formula (6), we find that, at this level of approximation, both approaches (i.e. with or without decomposing the magnetic excitation spectrum in two contributions) give the same correlation length and a slightly different energy width when the coupounds are located near the magnetic instability (that is to say for $J(\mathbf{Q})\,\chi_{SS}$ not too small).

Another difference between the canonical RPA expression and our dynamical susceptibility expression arises from the use of an energy ω_0 to

describe the data. The existence of the energy ω_0 is well established for the pure compound. For the compound studied here it is much more difficult to be affirmative on the existence of ω_0 because the ratio ω_0/Γ is smaller. This inelasticity is actually interpreted as a gap separating the collective non magnetic ground state from the magnetic excited state. Such an inelasticity is theoretically derived in a new approach of the Kondo lattice which treats the Kondo effect and the RKKY interactions on the same level.[24]

2. *Analysis in the Framework of the SCR Theory*

In a recent paper, T. Moriya and T. Takimoto[6] apply the SF theory known for 3d itinerant magnets to the heavy fermion case. The first step in their model is to compute a RPA dynamical susceptibility including SF renormalization. They then compute transport and thermodynamical properties. Following their notations, The main ingredients are two characteristic temperatures $T_A = Aq_B^2/2$ (characteristic SF in **Q** space) and $T_0 = T_A \Gamma_{SS}\chi_{SS}/\pi$ (characteristic SF in ω space). The dimensionless parameter, which determines the vicinity of the critical point, is $y_0 = 1/(2T_A\chi(\mathbf{k}))$ where $\chi(\mathbf{k})$ is the staggered susceptibility at the antiferromagnetic vector **k** at $T = 0$ K i.e. $1/\chi(\mathbf{k}) = 1/\chi_{SS} - J(\mathbf{k})$. At the magnetic instability $y_0 \to 0$, the NFL behaviour is reproduced by this model as characteristic of a crossover regime as for RG in 3 dimensions. A FL behaviour always persists at low enough temperature. S. Kambe *et al.*[7] apply this model to the heavy fermion compound $Ce_{1-x}La_xRu_2Si_2$ with $x = 0$, 0.05 and 0.075. They extract the parameters T_A, T_0, y_0 from the temperature dependence of the specific heat and compute the thermal expansion, resistivity and NMR relaxation rate. A general agreement is found for all of these physical quantities. On another hand, the agreement is less good when trying to compute the INS spectrum. We ascribe this difference to the fact that the INS results used in the paper of S. Kambe *et al.*[7] were extracted from a decomposition into single site and intersite signals giving rise to different characteristic parameters. A scaling factor was thus applied for a comparison between the INS data and the SCR parameters extracted from specific heat measurements. In the following, we extract the same characteristic SCR parameters at low temperature from the INS spectra at 1.5 K for $x = 0$ and $x = 0.075$, but we reanalyze them with the formula (10) in order to have exactly the same parameters as in the work of T. Moriya. In Fig. 9, we show the dispersion of $J(\mathbf{Q})\,\chi_{SS}$ around $\mathbf{k_2}$ for $x = 0$ and 0.075. This quantity is higher in the doped compound and its dispersion is stiffer. This is in agreement with the proximity of the magnetic instability. The parameters extracted from this analysis are shown in Table III.1 and compared with those determined by S. Kambe shown in Table III.2. We find a qualitative good

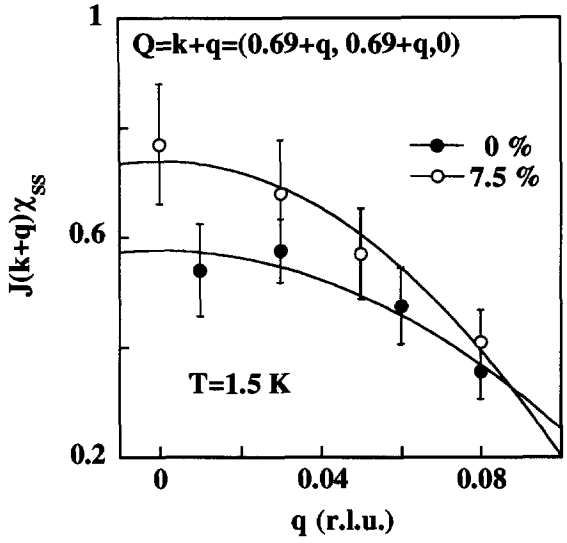

Fig. 9. Dependence in q of the quantity $J(\mathbf{k}+\mathbf{q})\chi_{SS}$ at $T = 1.5$ K derived from a RPA analysis of the data.

agreement between the parameters extracted from specific heat and INS measurements. Especially, the energy scales T_A and T_0 are of the same order of magnitude for both determination. The parameter y_0 indicating the proximity to the magnetic instability is also well reproduced. On another hand the parameter $J(\mathbf{k})$ is different. Some differences between the SCR model and the real magnetic excitation spectrum may explain this discrepency. Firstly, the SCR theory deals with an isotropic system whereas $CeRu_2Si_2$ is highly anisotropic. Secondly, the description is only valid around $\mathbf{Q} = \mathbf{k}$ and finally, in the real compound two vectors $\mathbf{k}_1$ and $\mathbf{k}_2$ exist. This phenomenological model is nevertheless useful in order to describe the location of these compounds in the critical phase diagram

TABLE III.1

SCR Parameters Extracted from INS Data at 1.5 K

	$x = 0$	$x = 0.075$
T_A (K)	11.3	11.0
T_0 (K)	14.2	16.5
$J(\mathbf{k})$ (meV)	3.3	2.5
y_0	0.23	0.07

TABLE III.2

SCR Parameters Extracted from Specific Heat After[7]

	$x=0$	$x=0.075$
T_A (K)	16	11
T_0 (K)	14.1	14.2
$J(\mathbf{k})$ (meV)	11	3.5
y_0	0.31	0.05

stressing the importance of spin fluctuations. Using macroscopic quantities such as specific heat it can also give an estimate of microscopic parameters like $J(\mathbf{k})$ and its dispersion which are directly probed by INS. This phenomenological approach is complimentary with the low statistics often characteristic of INS data. It is indeed much easier to extract some characteristic energies from the spectra than to extract the critical exponents. To this respect a comparison with the results dealing with the critical behaviour given in the recent review of Millis[5] is difficult. For example due to the limited statistics of the data in Fig. 7, we cannot give any definitive answer on the expected saturation of the correlation length at low temperature.

CONCLUSIONS

This study of $Ce_{0.925}La_{0.075}Ru_2Si_2$ points out the proximity of this compound to the magnetic instability. Compared to the pure compound, the energy widths are strongly reduced and the correlation length is larger. Thermal effects also appear at lower temperatures. This is in agreement with the increase of the RKKY interactions and the decrease of the Kondo temperature, upon going from $x=0$ to $x=0.075$. This behaviour is extensively explained by the SCR theory. There is indeed a qualitative agreement between the SCR parameters extracted from specific heat and INS measurements showing the importance of spin fluctuations in the physics of this class of compounds. Another important point is the occurrence of a tiny ordered moment at low temperatures which is usually reported for uranium based heavy fermions. This fact stresses the importance of defects in these family of alloys. It is obvious that more experiments are necessary, especially at low temperatures.

ACKNOWLEDGMENTS

We gratefully thank S. Pujol for technical assistance during the experiments at very low temperature on IN 12 at ILL. Ph. Boutrouille

gave precious cryogenic assistance at LLB. The help of B. Hennion allowed us to use the best experimental configuration on 4F2 at LLB. We thank B. Fåk for many useful and stimulating discussions. We gratefully acknowledge Brookhaven National Laboratory for its hospitality.

REFERENCES

1. J. Flouquet, S. Kambe, L. P. Regnault, P. Haen, J. P. Brison, F. Lapierre, and P. Lejay, *Physica B* **215**, 77 (1995).
2. R. A. Fisher, C. Marcenat, N. E. Phillips, P. Haen, F. Lapierre, P. Lejay, J. Flouquet, and J. Voiron, *J. Low Temp. Phys.* **84**, 49 (1991).
3. H. v. Löhneysen, T. Pietrus, G. Portish, H. G. Schlager, A. Schröder, M. Sieck, and T. Trappmann, *Phys. Rev. Lett.* **72**, 3262 (1994).
4. M. B. Maple, C. L. Seaman, D. A. Gajewski, Y. Dalichaouch, V. B. Barbetta, M. C. de Andrade, H. A. Mook, H. G. Lukefahr, O. O. Bernal, and D. E. Mac Laughlin, *J. Low Temp. Phys.* **95**, 225 (1994).
5. A. J. Millis, *Phys. Rev. B* **48**, 7183 (1993).
6. T. Moriya and T. Takimoto, *J. Phys. Soc. Jpn.* **64**, 960 (1995).
7. S. Kambe, S. Raymond, L. P. Regnault, J. Flouquet , P. Lejay, and P. Haen, *J. Phys. Soc. Jpn.* **65**, 3294 (1996).
8. L. P. Regnault, W. A. C. Erkelens, J. Rossat-Mignod, P. Lejay, and J. Flouquet, *Phys. Rev. B* **38**, 4481 (1988).
9. J. L. Jacoud, L. P. Regnault, J. Rossat-Mignod, C. Vettier, P. Lejay, and J. Flouquet, *Physica B* **156 & 157**, 818 (1989).
10. J. Rossat-Mignod, L. P. Regnault, J. L. Jacoud, C. Vettier, P. Lejay, J. Flouquet, E. Walker, D. Jaccard, and C. Amato, *J. Magn. Magn. Mat.* **76 & 77**, 376 (1988).
11. S. Quézel, P. Burlet, J. L. Jacoud, L. P. Regnault, J. Rossat-Mignod, C. Vettier, P. Lejay, and J. Flouquet, *J. Magn. Magn. Mat.* **76 & 77**, 403 (1988).
12. P. Lehman, Thesis, Strasbourg (1987).
13. P. Lejay, J. Muller, and R. Argoud, *J. Cryst. Growth* **130**, 238 (1993).
14. G. Aeppli, E. Bucher, C. Broholm, J. K. Kjems, J. Baumann, and J. Hufnagl, *Phys. Rev. Lett.* **60**, 615 (1988).
15. C. Broholm, J. K. Kjems, W. L. Buyers, P. Matthews, T. T. M. Palstra, A. A. Menovsky, and J. A. Mydosh, *Phys. Rev. Lett.* **58**, 1467 (1987).
16. A. Amato, R. Feyerherm, F. N. Gygax, A. Schenck, J. Flouquet, and P. Lejay, *Phys. Rev. B* **50**, 619 (1994).
17. F. Bourdarot, Thesis, Grenoble (1994).
18. A. de Visser, R. J. Keizer, A. A. Menovsky, M. Mihalik, F. S. Tautz, J. J. M. Franse, B. Fåk, N. H. v. Dijk, J. Flouquet, J. Bossy, and S. Pujol to be published in *Physica B, Proceedings SCES 1996.*
19. C. Di Castro and M. Grilli, in *Phase Separation in Cuprate Superconductors*, K. A. Müller and G. Benedek (Eds.), World Scientific, Singapore (1992).
20. J. L. Jacoud, Thesis, Grenoble (1991).
21. For an early discussion see R. A. Cowley, W. J. L. Buyers, P. Martel, and R. W. H. Stevenson, *J. Phys. C* **6**, 2997 (1973).
22. Y. Kuramoto, *Physica B* **156 & 157**, 789 (1989).
23. M. Loewenhaupt and K. H. Fischer, in *Handbook on the Physics and Chemistry of Rare Earths, Vol. 16*, Elsevier Science, Amsterdam (1993).
24. C. Pépin, Thesis, Grenoble 1996.